Magnetic and transport properties of the ferromagnetic semiconductor heterostructures (In,Mn)As/(Ga,Al)Sb

A. Oiwa, A. Endo, S. Katsumoto,* and Y. Iye*
Institute for Solid State Physics, University of Tokyo, Roppongi, Minato-ku, Tokyo 106-8666, Japan

H. Ohno
Research Institute of Electrical Communication, Tohoku University, Katahira, Aoba-ku, Sendai 980-8577, Japan

H. Munekata[†]
Imaging Science and Engineering Laboratory, Tokyo Institute of Technology, Nagatsuda 4259, Midori-ku Yokohama 226-8503, Japan

(Received 21 April 1998)

We have investigated the magnetic and transport properties of (In,Mn)As thin films grown on a (Ga,Al)Sb layer. Strong perpendicular magnetic anisotropy is observed for the (In,Mn)As layer, the thickness of which is less than the critical value required for relaxation of lattice-mismatch-induced strain. The anomalous Hall coefficient is found to be approximately proportional to the square of resistivity in the low-field region. Large negative magnetoresistance is found to occur over a magnetic field range significantly wider than that for the ferromagnetic hysteresis loop. [S0163-1829(98)04344-6]

I. INTRODUCTION

Recent developments in crystal growth of the III-V compound based magnetic semiconductor have offered great opportunities to study a variety of interesting phenomena arising from the interaction of carriers with local spins.[1–8] It has been established that (In,Mn)As and (Ga,Mn)As with a few percent of Mn exhibit ferromagnetic ordering at low temperatures.[2–9] Previous work on a series of $In_{0.94}Mn_{0.06}As/GaSb$ heterostructures has revealed that this ferromagnetic order is induced by the *p-d* exchange interaction between Mn spins and valence-band holes with concentration $\sim 2\times 10^{19}$ cm^{-3}.[8] The coupling between the Mn local spins and hole carriers also manifests itself in various spin-dependent magnetotransport phenomena.

The use of heterostructures provides additional means to control the relevant parameters, such as band offset and lattice matching. In this paper, we report on transport and magnetic properties of (In,Mn)As/(Ga,Al)Sb heterostructure systems. The system is isomorphic to InAs/GaSb, which has a so-called type-II band lineup, i.e., the GaSb valence-band top lies above the InAs conduction-band bottom.[10] The lattice mismatch is such that a tensile strain is exerted on the (In,Mn)As layer. It had been recognized earlier that the induced strain significantly influences the magnetic properties.[3,4] In the present work, we shed some light on this issue by investigating the relation between the magnetic anisotropy and film thickness. We also make a quantitative comparison of magnetization data with the Hall and magnetoresistance data, from which we discuss the mechanism of the anomalous Hall effect in this class of diluted magnetic semiconductors with relatively high Mn contents ($x>0.1$).

II. EXPERIMENT

Samples studied in this work were grown by molecular-beam epitaxy. The dependence of the physical properties of (In,Mn)As films on the growth parameters such as substrate temperature and Mn concentration has been previously reported.[1–3,5,6,8,9] The typical growth procedure is as follows. A GaSb buffer layer, approximately 0.3μm thick was first grown on top of a GaAs buffer layer on a semi-insulating GaAs(100) substrate. A (Ga,Al)Sb layer was then grown at 480 °C with thickness ranging from 0.14 to 1.3μm. Finally, an (In,Mn)As layer of thickness 9 or 20 nm was grown at 200 °C. Such a low growth temperature was chosen to avoid Mn segregation. In this paper, we report the results on three samples listed in Table I.

Magnetotransport measurements were carried out using a 15 T superconducting magnet with a variable temperature insert and a ^{3}He cryostat. A rotating sample holder was used to vary the magnetic-field direction with respect to the layer plane. In separate runs, we carried out the transport measure-

TABLE I. Parameters of the three $In_{1-x}Mn_xAs/Ga_{1-y}Al_ySb$ samples investigated. *d* is the thickness of the (In,Mn)As layer. The sheet resistance, hole density, and mobility are determined at 4.2 K.

Sample	x	y	d (nm)	Lattice mismatch (%)	ρ ($\Omega/\Box$)	p ($\times 10^{19}$ cm^{-3})	μ_p(cm^2/V s)
1	0.18	0.3	20	0.94	1570	1.9	105
2	0.12	0	9	0.70	1089	5.9	109
3	0.12	1	9	1.3	1082	4.5	144

0163-1829/99/59(8)/5826(6)/$15.00 ©1999 The American Physical Society

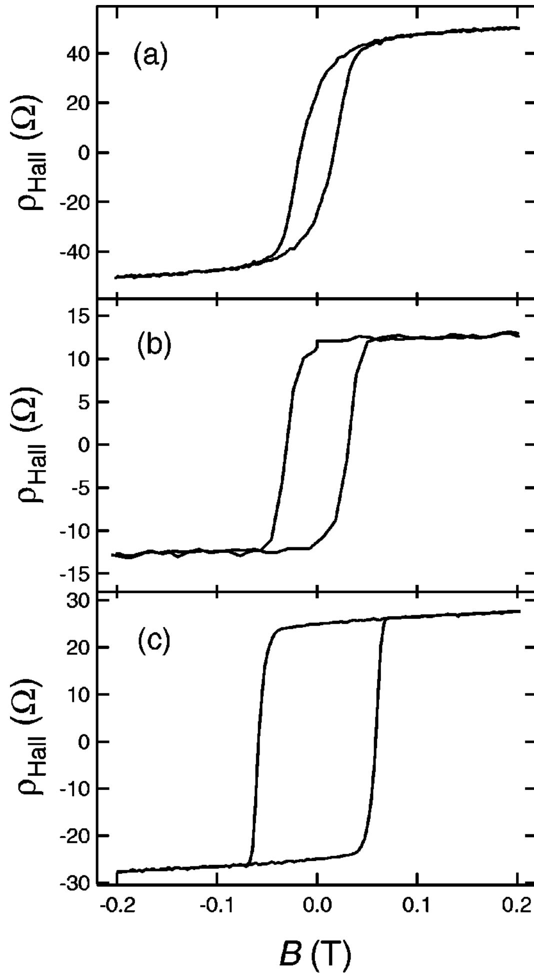

FIG. 1. Hall resistance in (a) Sample 1, $In_{0.82}Mn_{0.18}As$(20 nm)/$Ga_{0.7}Al_{0.3}As$; (b) Sample 2, $In_{0.88}Mn_{0.12}As$(9 nm)/GaSb; and (c) Sample 3, $In_{0.88}Mn_{0.12}As$(9 nm)/AlSb, in the low-magnetic-field region at 4.2 K showing magnetic hystresis. The magnetic field is applied perpendicular to the sample plane.

ments down to 40 mK using a dilution refrigerator. Magnetization measurements were done using a commercial SQUID magnetometer.

III. RESULTS AND DISCUSSION

A. Magnetic hysteresis and anisotropy

Figure 1 shows the low-field Hall resistance of the three samples at 4.2 K under perpendicular magnetic fields. The Hall resistance ρ_{Hall} of a magnetic semiconductor can be expressed phenomenologically as

$$\rho_{Hall} = \frac{R_0}{d} B + \frac{R_S}{d} M, \tag{1}$$

where d is the thickness of the magnetic layer. The first term on the right-hand side is the normal (or ordinary) Hall resistance and the second term represents the so-called anomalous (or extraordinary) Hall effect, which is proportional to the macroscopic magnetization M.[11] In the low-temperature and low-magnetic-field regime shown in Fig. 1, the Hall resis-

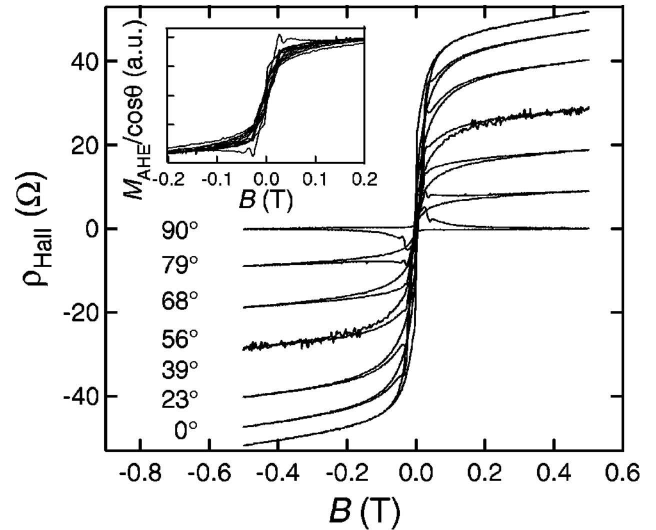

FIG. 2. Angular dependence of Hall resistance for the sample 1 [$In_{0.82}Mn_{0.18}As$(20 nm)/$Ga_{0.7}Al_{0.3}As$] at 4.2 K. Inset shows a scaling plot that demonstrates that the saturation magnetization is inverse proportional to cos θ.

tance is dominated by the anomalous component, and exhibits a hysteresis loop reflecting that of the ferromagnetic magnetization. The shape of the hysteresis loop in the Hall resistance quantitatively reproduces that of the magnetization measured by a SQUID magnetometer. This amounts to having a '' built-in'' magnetometer in each sample. This feature is quite advantageous in studying the ultrathin-film samples for which direct magnetization measurements are difficult.

It is seen in Fig. 1 that the hysteresis loops of the samples 2 and 3 are squarer in shape than that of 1. This suggests that the former samples have strong perpendicular magnetic anisotropy. The difference in the magnetic anisotropy is highlighted in Figs. 2 and 3, which show the dependence of the hysteresis loop on the angle of the applied magnetic field for

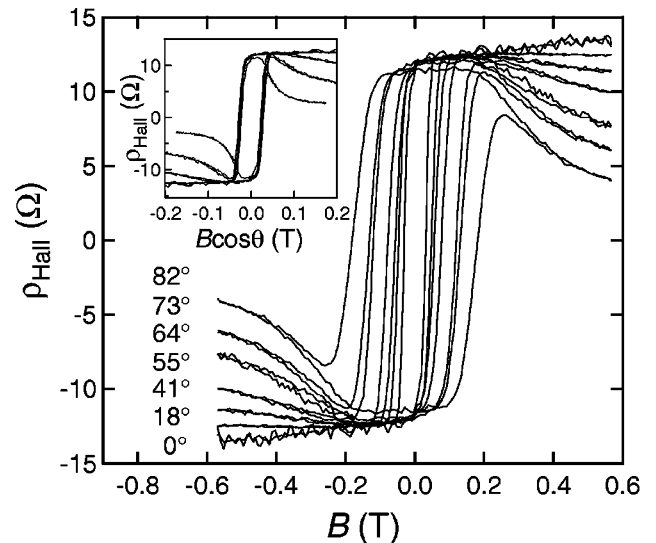

FIG. 3. Angular dependence of Hall resistance for the sample 2 [$In_{0.88}Mn_{0.12}As$(9 nm)/GaSb] at 4.2 K. Inset shows a scaling plot that demonstrates that the perpendicular field component $B \cos\theta$ determines the coercivity.

samples 1 and 2. The field angle θ is measured from the direction normal to the layer plane. In the sample 1 (Fig. 2), the magnitude of the saturation magnetization follows a cos θ dependence while the coercive force is nearly independent of θ. The inset shows a replot of the same data to highlight this scaling. Note that M_{AHE} means the magnetization deduced from the Hall resistance. The detail procedure to evaluate a magnetization from transport properties is discussed later. In the sample 2 (Fig. 3), on the other hand, the saturation magnetization is nearly independent of θ, while the coercive force is scaled by 1/cos θ as demonstrated in the inset.

The following picture emerges from these results: In sample 1, the magnetic anisotropy is relatively weak so that the magnetization follows the direction of the applied magnetic field. Sample 2, by contrast, has such a strong perpendicular magnetic anisotropy that the magnetization vector is always fixed normal to the layer plane, and only the perpendicular component of the applied magnetic field is effective. The negative slope of $\rho_{\mathrm{Hall}}(B)$ for larger θ values reflects the gradual tilting of the magnetization vector from the plane normal towards the direction of the applied field with increasing field strength.

We attribute the difference in magnetic anisotropy to the lattice-mismatch-induced strain in the magnetic layer.[3] In the case of sample 1, the thickness of the magnetic layer exceeds the critical value for introduction of dislocations, so that the lattice-mismatch-induced strain is mostly relaxed. By contrast, the magnetic layers in samples 2 and 3 are thinner than the critical thickness, and are highly strained, giving rise to the observed perpendicular magnetic anisotropy. Of samples 2 and 3, the latter has a larger coercive force because of the larger lattice-mismatch of the (In,Mn)As layer with the AlSb underlayer than with the GaSb underlayer. Thus, we believe the lattice-mismatch-induced strain is the principal source of the magnetic anisotropy, although other factors such as carrier density and dislocation density have to be considered for quantitative account of the phenomenon.

The difference in the magnetic anisotropy is also reflected in the behavior of nonequilibrium magnetization. Figure 4(a) shows the temporal relaxation of the remanent magnetization (as detected by the Hall resistance) of sample 1 at $T=2.1$ K. The data were taken at zero field after a field excursion up to 1 T. This logarithmic relaxation phenomenon and the relatively narrow and rounded hysteresis loop [Fig. 1(a)] suggest that the Mn moments form ferromagnetic clusters that act as giant spins.[2] The fact that magnetization relaxation can be observed at such low temperatures indicates the superparamagnetic character of these giant spins. In other words, the weakness of magnetic anisotropy in this sample allows relatively free rotation of the giant spins. This sort of logarithmic time relaxation is known to occur in a superparamagnet with distributed cluster sizes.[12] Figure 4(b) shows similar data for sample 2 at $T=20$ K, which is lower by about 15 K than the Curie temperature. Because this sample has much larger magnetic anisotropy, the magnetic relaxation cannot be observed at low temperatures. It is only at such high temperatures that the relaxation time scale comes into the experimental time window. In the case of sample 3, which is most anisotropic, the logarithmic time dependence of magnetization was observable only at still higher temperature near the ferromagnetic transition ($T_C \approx 35$ K).

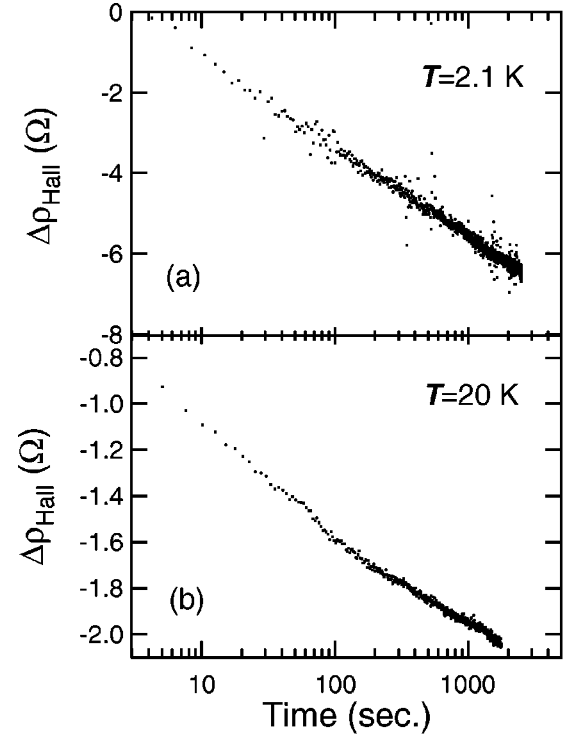

FIG. 4. Temporal relaxation of zero-field Hall resistance in (a) sample 1 [$In_{0.82}Mn_{0.18}As$(20 nm)/$Ga_{0.7}Al_{0.3}Sb$] at 2.1 K and (b) sample 2 [$In_{0.88}Mn_{0.12}As$ (9 nm)/GaSb] at 20 K, after the magnetic field cycling to 1 T. The quantity $\Delta\rho_{\mathrm{Hall}}$ is the deviation from the value right after the sweepdown of the magnetic field. The logarithmic time relaxation of magnetization is seen over a wide time span.

B. Temperature dependence of magnetization and mechanism of anomalous Hall effect

As mentioned in the previous subsection, the anomalous Hall term quantitatively reproduces the shape of the ferromagnetic hysteresis loop at a given temperature. Here we look into the temperature dependence of the relationship between the anomalous Hall term and the magnetization. This was brought to our attention by the observation that the low-field Hall resistance increases steeply as $T \rightarrow 0$. In the light of Eq. (1), this temperature dependence should be attributed to that of the coefficient R_S. Conventionally, two types of process are invoked for the mechanism responsible for the anomalous Hall effect.[11] One is the skew scattering process and the other is the side-jump process. The anomalous Hall coefficient R_S is directly proportional to ρ in the former case, while it is proportional to ρ^2 in the latter case. The resistivity ρ in the present samples is governed by the scattering by the magnetic impurities. As shown in Table I, the carrier mobility is fairly low, and the estimated mean free path is comparable to the average Mn distance.

Figure 5 shows comparison of the temperature dependence of magnetization in sample 3 deduced from the anomalous Hall effect with that directly measured by the SQUID magnetometer. The absolute value of the magnetization obtained from the anomalous Hall effect is scaled to fit to the SQUID data at $T=25$ K. The solid squares represent those calculated by assuming the skew scattering mechanism ($R_S \propto \rho$), while the solid circles are those based on the side-

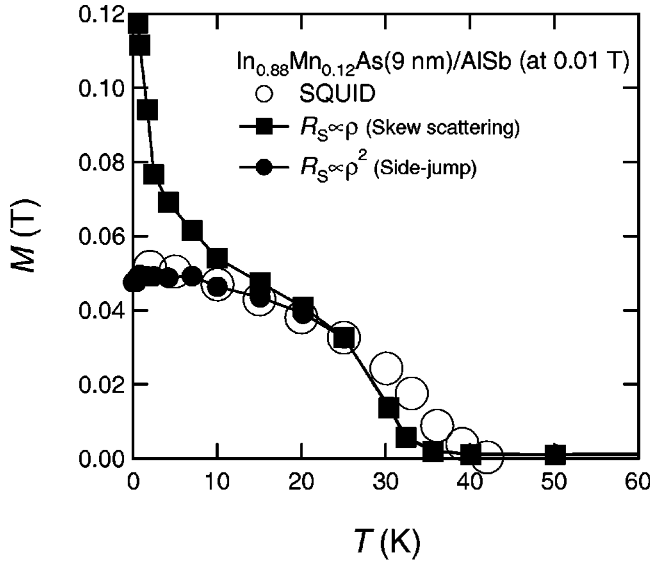

FIG. 5. Temperature dependence of magnetization at 0.01 T for sample 3 [$In_{0.88}Mn_{0.12}As$(9 nm)/AlSb]. The open circles show the magnetization measured by a SQUID magnetometer. The solid squares and solid circles represent the magnetization deduced from the Hall resistance, assuming $R_S \propto \rho$ (skew scattering) or $R_S \propto \rho^2$ (side jump), respectively.

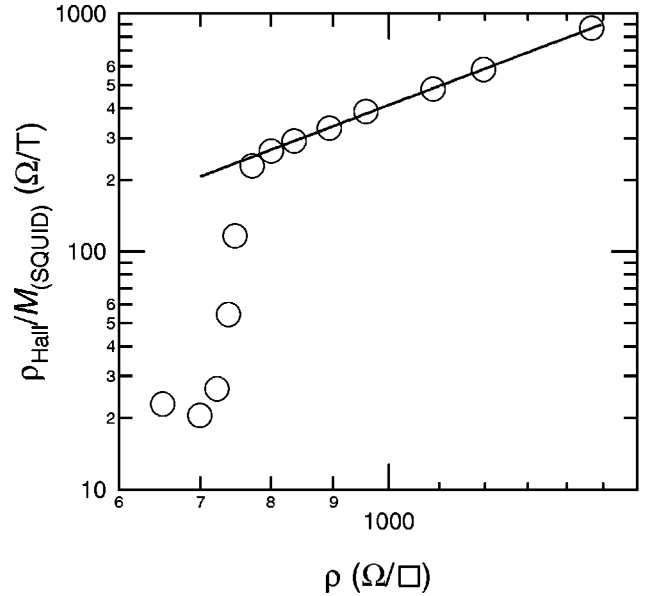

FIG. 6. Anomalous Hall coefficient $R_S(=\rho_{Hall}/M_{(SQUID)})$ vs sheet resistance ρ in a log-log plot for sample 3 [$In_{0.88}Mn_{0.12}As$(9 nm)/AlSb]. The solid line represents a power-law relation, $R_S \propto \rho^{1.9}$.

jump mechanism ($R_S \propto \rho^2$). As seen clearly, the analysis based on the assumption $R_S \propto \rho$ leads to an unnatural increase in magnetization at low temperatures, which disagrees with the SQUID data. On the other hand, the solid circles evaluated by assuming $R_S \propto \rho^2$ show reasonable agreement with the SQUID data. The experimental data for the other two samples are similar in that they yield an unphysical increase of magnetization at low temperatures if $R_S \propto \rho$ is assumed, while they give a more or less reasonable behavior if $R_S \propto \rho^2$ is employed.

To be more quantitative, Fig. 6 shows a log-log plot of R_S vs ρ in sample 3. Here, R_S is evaluated from $\rho_{Hall}/M_{(SQUID)}$ at $B=0.01$ T, because the first term in Eq. (1) is negligible there. Different points represent data at different temperatures. The data below about 25 K appear to obey a power-law relation, $R_S \propto \rho^{1.9}$. Thus, the present results seem to suggest that the side-jump mechanism plays an important role in the asymmetric scattering process in this class of materials at least in the temperature region below the Curie temperature (~35 K for sample 3). Deviation from this power-law relation is observed above ~25 K.

Generally stated, the side-jump mechanism may gain relative importance over the skew scattering mechanism in a system with shorter mean free path, i.e., higher Mn concentration. This is because, for the skew scattering to be effective, the deflected carrier has to travel a considerable distance before it is scattered by another Mn moment.[11] In fact, the skew scattering seems to be important in a sample with lower Mn concentration.[2]

Returning to Fig. 5, the saturation magnetization at $B=0.01$ T extrapolated to $T=0$ K is found to be only about 40% of the full saturation value $M_S \approx 0.12$ T estimated by assuming $S_{Mn}=5/2$. In other words, only about 40% of the Mn spins apparently participate in the low-field ferromagnetism. The implication of this observation will be discussed in the next subsection.

C. High-field behavior and large negative magnetoresistance

Figure 7 shows the Hall and magnetoresistance in sample 3 over a wide magnetic field range at different temperatures. The other two samples behave in similar fashions. The Hall resistance ρ_{Hall} shows a hysteresis loop at low fields and low temperatures as we have already seen in Fig. 1(c). The amplitude of the hysteresis is seen to increase with decreasing temperature. This is linked to the unusual behavior represented by the solid squares $\propto R_{Hall}/\rho$ in Fig. 5. The $\rho_{Hall}(B)$ curve shows a characteristic overshoot before it tends to a straight line at high magnetic fields. The longitudinal resistance $\rho(B)$ shows a very large negative magnetoresistance in the same field range. The negative magnetoresistance grows rapidly with decreasing temperature. The overshoot of the $\rho_{Hall}(B)$ curve is evidently related to the large negative magnetoresistance. In fact, if we plot ρ_{Hall}/ρ^2 as a function of B, the overshoot becomes much reduced and the resultant curve is closer to the $M(B)$ curve. But even then, the two curves do not completely agree with each other. The agreement can be certainly improved, if ρ is replaced with $\rho-\rho_0$ with ρ_0 representing the scattering rate irrelevant to the anomalous Hall effect. This, however, practically amounts to introducing another fitting parameter, and therefore the resulting better fitting may contribute little to physical insight unless the physical process behind the parameter is clearly specified.

As mentioned in the previous subsection, only about 40% of the total Mn spins appears to participate in the low-field ferromagnetic hysteresis loop. The remaining Mn spins require much higher field to align. The reason for the existence of the nonferromagnetic Mn spins may be firstly sought in the depletion layer region where the hole density can be

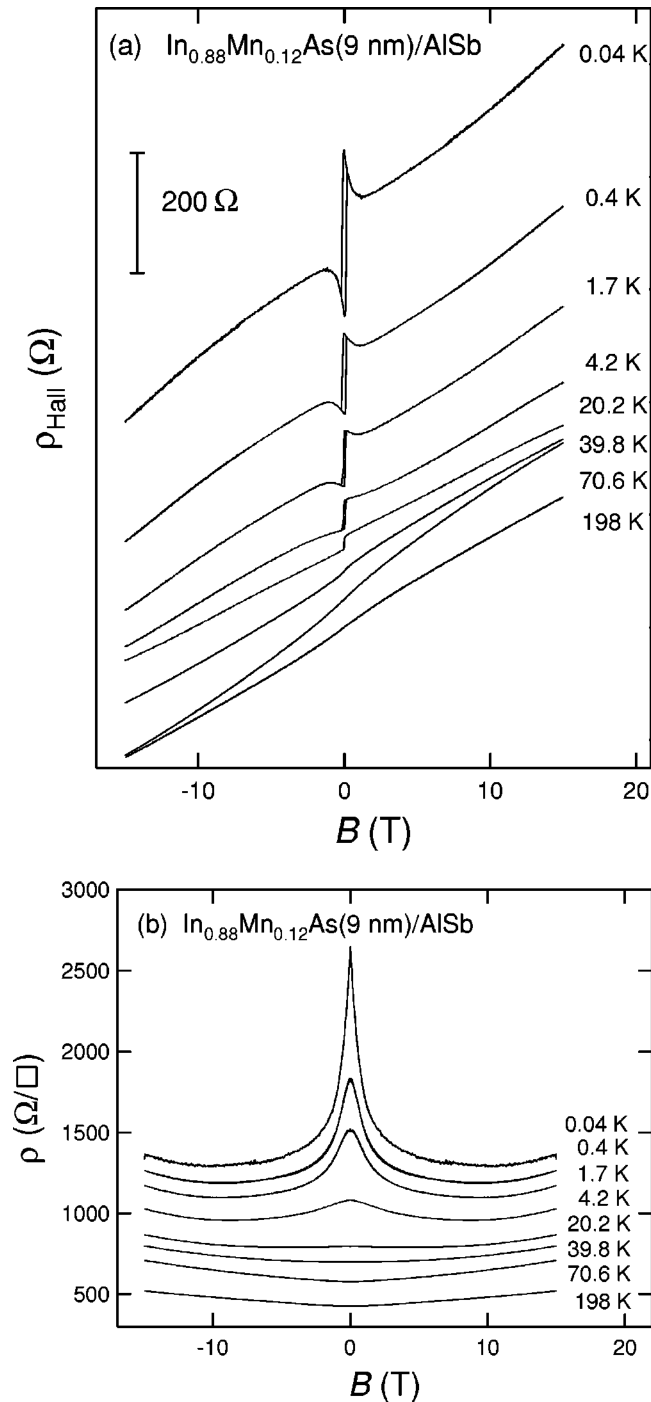

FIG. 7. (a) Hall resistance and (b) magnetoresistance of sample 3 [$In_{0.88}Mn_{0.12}As$ (9 nm)/AlSb] at different temperatures. The Hall resistance curves are vertically shifted for clarity.

lower than the critical value for the occurrence of carrier-induced ferromagnetism. This accounts for a certain fraction of the nonferromagnetic Mn spins, but not all, because similar phenomena are also observed in thick film samples. Therefore, at least some part of the nonferromagnetic Mn spins do coexist with the ferromagnetic clusters in the interior of the (In,Mn)As layer.

The direct exchange between neighboring Mn spins is known to be antiferromagnetic. A significant fraction of the Mn spins showing the nonferromagnetic behavior, therefore, are thought to take random antiferromagnetic configuration. The observed large negative magnetoresistance is presumably related to gradual alignment of such Mn spins. For (Ga,Mn)As thick films, such gradually saturating magnetization component is actually observed by direct magnetization measurements.[13] Although such direct magnetization measurements have not been done on these particular samples of (In,Mn)As, the overall similarity of the magnetotransport behavior strongly suggests that the similar picture holds. At still higher fields, the magnetoresistance turns to positive. This small positive magnetoresistance at higher fields is attributed to the ordinary classical magnetoresistance due to the Lorentz force.

Before concluding, a word on the possibility of parallel conduction is due. Throughout the above discussions, we have assumed that the conduction is solely carried by the (In,Mn)As layer. Given the heterostructure of the present samples, there is some possibility that a conducting p channel exists on the (Ga,Al)Sb side of the heterointerface. We believe, however, that such a parallel conducting channel, if it exists, plays only a minor role in the present systems. The valence band offset at the InAs/(Ga,Al)Sb interface varies from $\Delta E_v \approx 0.48$ eV for InAs/GaSb to ≈ 0.08 eV for InAs/AlSb.[14] Therefore, the formation of a p-type conduction channel on the (Ga,Al)Sb side of the interface and its contribution to the transport are expected to differ widely among the samples with different alloy composition. On the other hand, the present three samples have similar resistivity values as shown in Table I, and their magnetotransport behaviors are also similar to one another. This seems to indicate that as far as the present samples are concerned the conduction is dominated by the (In,Mn)As layer, and that the contribution from the parallel conducting channel is small, if any. The possibility of contribution from the parallel conduction channel, however, should be always borne in mind in this class of systems.

IV. CONCLUSION

We have investigated the magnetic and transport properties of (In,Mn)As thin-film samples in their ferromagnetic phases at low temperatures. The Hall resistance is dominated by the anomalous Hall effect, so that it reflects the behavior of magnetization. The magnetic anisotropy that is deduced from the dependence of the hysteresis loop on the field angle exhibits distinct difference between the thinner ($d = 9$ nm) and the thicker ($d = 20$ nm) samples. The most plausable souce of the difference is the lattice-mismatch-induced strain in the former and its relaxation in the latter. Comparison with the SQUID data indicates that the anomalous Hall coefficient is proportional to ρ^2 rather than ρ, suggesting the side-jump process as the dominant mechanism for the asymmetric scattering of carriers. The ferromagnetically aligned Mn spins form clusters. In the least anisotropic sample (1), those ferromagnetic clusters exhibit superparamagnetic behavior, as suggested by the rounded magnetization curve and long-term relaxation at very low temperatures. A large negative magnetoresistance is observed over a field range much wider than the ferromagnetic hysteresis. Such high-field behavior is correlated with the gradual alignment of Mn spins that do not participate in the low-field ferromagnetic hysteresis.

ACKNOWLEDGMENTS

The authors thank H. Takagi and K. Nozawa of ISSP for their help with the SQUID measurements. This work was partly supported by a Grant-in-Aid for the Scientific Research on Priority Area ''Spin Controlled Semiconductor Nanostructures'' from the Ministry of Education, Science, Sports and Culture, Japan. One of the authors (H.M.) acknowledges support by the TORAY Science Foundation, the TEPCO Research Foundation, and Kanagawa Academy of Science and Technology.

*Also at CREST, Japan Scicence and Technology Corporation, Japan.

†Also at PRESTO, Japan Science and Technology Corporation, Japan.

[1] H. Munekata, H. Ohno, S. von Molnar, A. Segmüller, L. L. Chang, and L. Esaki, Phys. Rev. Lett. **63**, 1849 (1989).

[2] H. Ohno, H. Munekata, T. Penney, S. von Molnar, and L. L. Chang, Phys. Rev. Lett. **68**, 2664 (1992).

[3] H. Munekata, A. Zaslavsky, P. Fumagalli, and R. J. Gambino, Appl. Phys. Lett. **63**, 2929 (1993).

[4] H. Munekata, in *Proceedings of 22nd International Conference on Physics of Semiconductors, Vancouver, 1994*, edited by D. J. Lockwood (World Scientific, Singapore, 1995), p. 2517.

[5] H. Munekata, Mater. Sci. Eng., B **31**, 151 (1995).

[6] H. Ohno, F. Matsukura, H. Munekata, Y. Iye, and J Nakahara, in *Proceedings of the 22nd International Conference on the Physics of Semiconductors, Vancouver, 1994*, edited by D. J. Lockwood (World Scientific, Singapore, 1995), p. 2605.

[7] H. Ohno, A. Shen, F. Matsukura, A. Oiwa, A. Endo, S. Katsumoto, and Y. Iye, Appl. Phys. Lett. **69**, 363 (1996).

[8] H. Munekata, T. Abe, S. Koshihara, A. Oiwa, M. Hirasawa, S. Katsumoto, Y. Iye, L. Urano, and H. Takagi, J. Appl. Phys. **81**, 4862 (1997).

[9] A. Shen, F. Matsukura, Y. Sugawara, T. Kuroiwa, H. Ohno, A. Oiwa, A. Endo, S. Katsumoto, and Y. Iye, Appl. Surf. Sci. **113-114**, 183 (1997).

[10] L. L. Chang and L. Esaki, Surf. Sci. **98**, 70 (1980).

[11] C. M. Hurd, *The Hall Effect and Its Application*, edited by C. L. Chien and C. R. Westgate (Plenum, New York, 1980), p. 3.

[12] L. Neel, Ann. Geophys. (C.N.R.S.) **5**, 99 (1949).

[13] A. Oiwa, S. Katsumoto, A. Endo, M. Hirasawa, Y. Iye, H. Ohno, F. Matsukura, A. Shen, and Y. Sugawara, Solid State Commun. **103**, 209 (1997).

[14] L. F. Luo, R. Beresford, and W. I. Wang, Appl. Phys. Lett. **55**, 2033 (1989), and references therein.